Fast climate impact emulation for global temperature scenarios with the Rapid Impact Model Emulator (RIME)

Edward Byers [1]*, Michaela Werning [1], Mahé Perrette [2], Niklas Schwind [1], Volker Krey [1], Keywan Riahi [1] & Carl-Friedrich Schleussner [1, 3]

[1] Energy, Climate and Environment Program, International Institute for Applied Systems Analysis, Schlossplatz 1, 2361 Laxenburg, Austria
[2] Alfred Wegener Institute, Telegrafenberg A 45, 14473 Potsdam, Germany
[3] IRI THESys, Humboldt-Universität zu Berlin, Unter den Linden 6, 10099 Berlin, Germany

* Corresponding author: byers@iiasa.ac.at

Abstract

Climate model emulation has long been applied to assess the global climate outcomes of integrated assessment model (IAM) emissions scenarios, but is typically limited to first-order climate variables like mean surface air temperatures at limited regional resolution. Here we introduce RIME, the Rapid Impact Model Emulator, which uses global warming level interpolation approaches based on inputs of global mean air temperature pathways to calculate a range of climate impact driver (CID) indices and exposure metrics. The emulation is fast and versatile, producing batches of CID indices and exposure metrics to complement IAM scenarios thereby bridging the IPCC impacts (WGII) and mitigation (WGIII) communities. Our lightweight emulator produces both gridded and regionally-aggregated results taking us beyond the computationally-intensive constraints of global earth system and impact models. The approach allows to assess the combined outcome of a wide range of emission and socio-economic scenarios enabling a decomposition of drivers of uncertainty for future climate risks. While climate uncertainties are the primary concern through mid-century, our results indicate that socio-economic factors such as population growth may become the dominant drivers of risk by the end of the century. We demonstrate an application to IPCC scenarios to illustrate its potential utility while acknowledging methodological constraints and delineating a comprehensive roadmap for future development. These rapid climate risk emulation frameworks exhibit significant promise for facilitating cross-disciplinary integration and enhancing scientific inclusivity across diverse research communities.

1 Introduction

There is growing demand across research, policy, business and civil society for a more agile exploration of climate hazards and impacts under varied emission and socio-economic scenarios (Tebaldi et al., 2025) to answer questions such as ‘How will heatwaves change by 2050 under current climate policies?’, or ‘What impacts are avoided if we mitigate consistent with the 1.5 °C pathways identified in the latest report of the Intergovernmental Panel on Climate Change?’ State-of-the-art, complex earth system models (ESMs) simulate the earth’s atmosphere, land surface, oceans, cryosphere, carbon and bio-geochemical cycles in spatial detail and at daily resolution. However, ESM simulations require supercomputers, weeks to months of runtime, and generate vast data volumes. Thus, ESMs are typically constrained to running tens of scenarios in highly structured, community-driven model intercomparison exercises, like the ScenarioMIP activity (van Vuuren et al., 2025) of the Coupled Model Intercomparison Project (CMIP)(Eyring et al., 2016), a process which from initial scenario design to complete assessment in IPCC Working Group 1 (WGI) (Masson-Delmotte et al., 2021), takes over five to seven years. More rapid assessments are thus needed and are gaining traction (Forster et al., 2025; Tebaldi et al., 2025).

In response, development and use of simple climate models (SCMs) and climate model emulators has accelerated. SCMs efficiently simulate global climate responses to radiative forcing or emissions scenarios, primarily reporting annual global mean surface temperature (GMT). Their speed enables efficient exploration of long-duration scenarios, many varied emissions pathways and probabilistic assessments sampling parametric uncertainties, making them central to integrated assessment modelling. Examples include FaIR (Smith et al., 2018), MAGICC (Meinshausen et al., 2011), OSCAR (Gasser et al., 2017; Quilcaille et al., 2023a), HECTOR (Dorheim et al., 2024) and CICERO-SCM (Sandstad et al., 2024), which featured in the Reduced Complexity Model Intercomparison Project (RCMIP - Nicholls et al., 2020), as well as IPCC WGIII’s (Riahi et al., 2022) climate assessment (Kikstra et al., 2022) of the mitigation scenarios database (Byers et al., 2022).

Assessing the regional climate impact outcomes of many different emissions scenarios is obviously also of particular interest, but not feasible in neither SCMs nor ESMs. Yet, many climate variables and impacts scale with global mean temperature (GMT), enabling regional projections based on global warming levels. Pattern scaling (Frieler et al., 2012; Tebaldi et al., 2020) assumes linear relationships between local variables and GMT, performing well for temperature but less so for precipitation due to non-linearities and regional forcings (Myhre et al., 2018). The time-slicing (James et al., 2017) of climate impacts at fixed GMT thresholds (e.g., 1.5 °C, 2 °C), is grounded in the concept of the transient climate response to cumulative emissions (Allen et al., 2009) and avoids assuming functional dependencies of pattern scaling. This method has gained traction in climate impact studies (Piontek et al., 2014; Schleussner et al., 2016; Byers et al., 2018, p. 201; Lange et al., 2020; Werning et al., 2024b; Tebaldi and Knutti, 2018) and featured prominently in the Special Report on Global Warming of 1.5°C and in the 6th Assessment Reports of the Intergovernmental Panel on Climate Change (IPCC) (Hoegh-Guldberg et al., 2018; IPCC, 2023). However, both approaches primarily assess average climate responses, while important insights on climate variability are lost.

Recent developments in spatially explicit ESM emulators aim to address this gap by rapidly reproducing or generating multiple climate variables and indicators, including variability. STITCHES (Tebaldi et al., 2022) uses time-slicing (James et al., 2017) and warming rates to reproduce any variable from archived ESM output by stitching together samples from different runs. MESMER (Beusch et al., 2020) takes the regional response through global mean temperature pattern scaling while introducing natural variability through stochastic processes to generate new timeseries. Whilst STITCHES can rapidly reproduce multi-variate variables from the ESM output archive, MESMER requires a bespoke calibration process per variable. These have been applied to annual (Beusch et al., 2020; Quilcaille et al., 2022) and monthly temperatures (Nath et al., 2022), fire weather and soil moisture (Quilcaille et al., 2023b), and joint emulation of temperature and precipitation (Schöngart et al., 2024). MERCURY (Nath et al., 2024) extends the MESMER methods in a multi-variate manner for the humid-heat metric of wet-bulb globe temperature using a memory-efficient data compression and lifting scheme, while QuickClim (Kitsios et al., 2023), applies machine learning based on CO_2 concentrations, bypassing GMT and enabling multivariate emulation of seven key ESM outputs.

Ultimately, these approaches extend the post-processing chain from integrated assessment model (IAM) emissions scenarios to global mean temperatures and then to spatial climate variables, enabling the calculation of indicators and extremes. However, currently attention tends to be on first-order ESM outputs like mean air temperatures and precipitation, with much of the development and progress focused on introducing annual and monthly variability, or on understanding performance under low emissions scenarios, aerosol forcing or overshoot conditions (Schwaab et al., 2024). And whilst some efforts target indicators derived from the ESM variables, development of new indicators remains resource intensive and without further post-processing, somewhat limits these emulators' ability to assess socioeconomic risks of climate change in a timely manner.

Here, we demonstrate a workflow to complement this area of research with a climate impact emulator coupled with a broader range of Climate Impact Driver (CID) indices and exposure metrics (Figure 1), which we refer to here more generally as indicators. CIDs, which were developed alongside Working Group I of the IPCC 6th Assessment Report, are specific physical climate conditions, like extreme heat or sea-level rise, that directly affect elements of society or ecosystems (Ruane et al., 2022). There are seven overarching CID types (heat and cold, wet and dry, wind, snow and ice, coastal, open ocean, and other), comprising a total of 33 CID categories which may be measured by a variety of indices. Here, we use also CID exposure metrics to measure the exposure of society or ecosystems to a CID index above a threshold.

The approach uses global warming level methods on CID indices combined into a workflow and software package called the Rapid Impact Model Emulator (RIME). RIME takes a GMT pathway, e.g. from an IAM+SCM scenario, combined with a CID indices database, to calculate CID index and exposure metrics based on the GMT pathway. In this case we use CID indices calculated from model outputs of the Inter-Sectoral Inter-Model Intercomparison Project (ISIMIP) (Werning et al., 2024b, 2024a). ISIMIP comprises a suite of consistently bias-adjusted and downscaled (Lange, 2019) ESM datasets from the ScenarioMIP (O'Neill et al., 2016), as well as climate impact model results which take the ESM datasets as forcing inputs and are run using a common protocol (Frieler, 2024). The RIME workflow is designed to be fast and versatile, producing batches of indicators for a wide range of global warming scenarios. The approach and outputs are not directly comparable, but complementary to the aforementioned ESM emulators. RIME intentionally pushes forwards through the climate impacts chain to produce multiple, independent CID index and exposure metrics for different global warming pathways. Thus, the complexity is currently reduced, for example by not yet including inter-annual variability, for the sake of providing transient CID indices and exposure metrics more broadly suitable for integrated assessment modelling (see section 4).

Broadly, RIME aims to meet needs for climate impacts frameworks that are lightweight and offer scenario flexibility, for applications such as rapid risk screening in regional planning, corporate risk assessment and disclosure, climate education and inter-disciplinary research. For example, the approach will feature in the forthcoming 7th Global Environment Outlook report of the United Nations Environment Programme whilst a more advanced methodology is in development (Schwind, 2025) and will be used in the Climate Impacts Explorer of the Network for Greening the Financial System (NGFS) (https://climate-impact-explorer.climateanalytics.org/).

The motivation for this approach and accompanying software was to operate at the interface between the climate impacts and climate mitigation communities. Within the Intergovernmental Panel for Climate Change (IPCC), this is the interface between working groups II and III, whilst global research communities primarily include ISIMIP ("ISIMIP," 2024) and the Integrated Assessment Modelling Consortium (IAMC, ("IAMC," 2024)). Data formats and conventions are thus intended to be well aligned with these communities. Depending on the inputs available and outputs required, both gridded maps and regional table data can be produced. In this specific context, there are two key use cases intended: i) post-processing, such that global integrated assessment model scenarios with temperature pathways can be rapidly complemented by a suite of climate impact and exposure indicators to facilitate the comparison of mitigation strategies with incurred impacts; and ii) impacts integration, such that climate impacts are integrated into quantitative scenarios, either through the pre-processing of input data, or endogenously into a model framework so that impacts are assessed on the fly. The rest of this paper describes the methodology, typical workflow and use cases, illustrates the functionality, and concludes with a discussion on limitations and directions for further development and use cases.

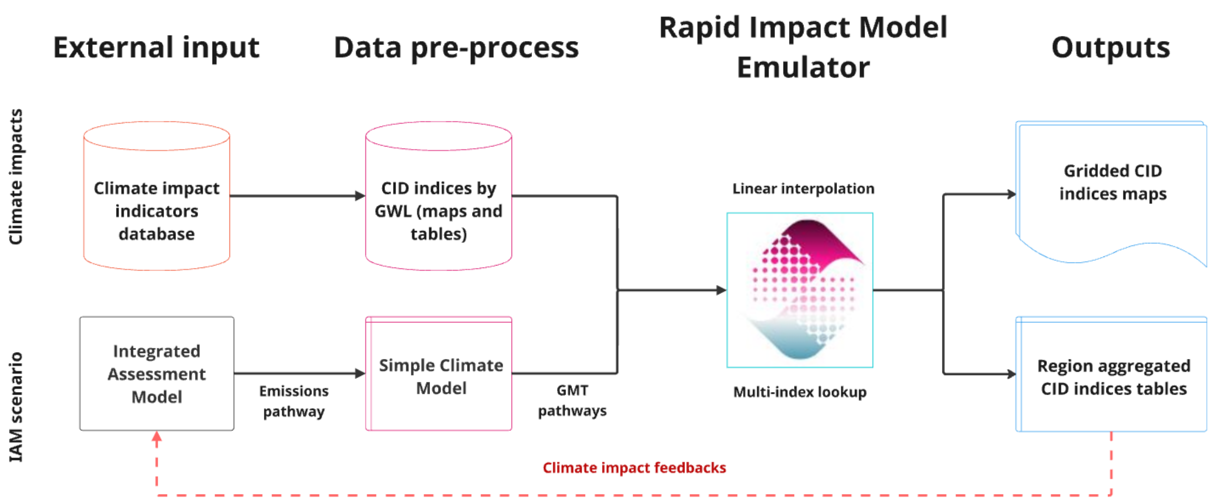

Figure 1. Overview of the general workflow, primarily from the perspective of the IAM scenario post-processing, use case (i). The red feedback line indicates the use case of climate impacts integration into integrated assessment modelling, use case (ii).

2 Methodology

2.1 Background

Within RIME, input data is provided at GWLs, obtained through temperature time-slicing, thus providing an empirical map of CID indices onto GWLs that, unlike normal pattern-scaling (Wells et al., 2023), does not require the assumption of linearity. Only subsequently are intermediate values linearly interpolated. An assumption or knowledge of an underlying functional form is not required, thereby allowing RIME to be applied with any impact indicator that is mainly dependent on the global mean temperature level and the provided socioeconomic data.

2.2 Workflow overview

The approach for using RIME requires broadly the following steps:

1. Input pre-processing: a (time-sampled) input database of CID indices and exposure metrics data by global warming levels (GWLs) and socioeconomic scenarios, which can be both gridded and tabular regional inputs. Default temperature resolution as used here is 0.5 °C, although finer resolution is also possible. Gridded inputs are called raster arrays. Table inputs, which would have values aggregated to a region (e.g. country, IPCC climate zone, etc.), are called region arrays.
2. Linear interpolation: the datasets are linearly interpolated between GWLs to high resolution (e.g. 0.01 or 0.05 °C), whilst other dimensions, which could be non-numeric and categorical, e.g. a socioeconomic dimension (e.g. SSP), can be preserved discreetly. This forms the input database, which depending on the application, can be interpolated for everything a priori albeit with high storage requirements, or on-the-fly when only specific variables are required.
3. Multi-index lookup: taking the GMT timeseries for the input IAM scenario (a GMT pathway), a multi-index lookup for each timestep (year) to identify the closest GWL and (if relevant) socioeconomic

scenario, is performed on the input database, to develop a continuous timeseries of climate impacts data consistent with the warming pathway.

Parallelization of this workflow, which combines drawing on heavy input datasets with multiple indicators with the need to potentially process 10s or even 100s of GMT pathways, is thus necessary and feasible. Within RIME, the current implementation enables parallelized processing in the following modalities (with the possibility of further development extensions):

1. Multi-scenario mode: multiple GMT pathways are input, with one indicator processed for all pathways in parallel. For example, for 5 (or 500) IAM scenarios, this mode provides results of one CID index for comparison across the ensemble of GMT pathways from the IAM scenarios.
2. Multi-indicator mode: in this case, one GMT pathway is processed, with the calculation of multiple indicators occurring in parallel. For example, for one GMT pathway (from and IAM scenario), this mode provides datasets with multiple CID indices and exposure metrics etc.

The two use cases above can also be combined such that multiple scenarios are processed for multiple indicators, which is implemented by parallelizing the processing of multiple scenarios using the multi-indicator mode (2). In any case, CID indices and exposure data for each scenario are subsequently calculated in the order of seconds to minutes on a desktop workstation, depending on the number of indicators and temporal resolution.

To provide a more contextually informative description of the methodology, the sections that follow describe the implementation as tested and described using a climate impact indicators dataset (Werning et al., 2024b, 2024a) based on ISIMIP3b datasets. It is noted that other input datasets mapped by global warming levels are expected to work and could include, for example, wider sets of indicators or inputs from other impacts models. In comparison of indicators, it is important to aim for consistency in how they are calculated.

2.3 Pre-processing the climate impacts input database

A database of climate impact driver indices (CID indices) (Werning et al., 2024b, 2024a) calculated from the bias-adjusted and downscaled outputs of global CMIP6 ESMs and global hydrological models is used. From this database we use primarily 9 CID indices (with many more variants) spanning six categories across the "Heat and cold" and "Wet and dry" CID types, covering extremes in precipitation and air temperatures, wet-bulb temperature heatwaves, cooling degree days, and the drought intensity, seasonality and inter-annual variability of runoff and discharge.

Table 1. Overview of model datasets used and CID indices tested in this workflow and as available and described in Table S 1 and (Werning et al., 2024b, 2024a), organized by the CID framework (Ruane et al., 2022).

<table>
<tr><th>CID type</th><th>CID category</th><th>Models</th><th>CID indices (# of variants)</th></tr>
<tr><td rowspan="2">Heat and Cold</td><td>Mean air temperature</td><td rowspan="2">Five ISIMIP3b bias-adjusted and downscaled CMIP6 ESM datasets:

GFDL-ESM4
IPSL-CM6A-LR
MPI-ESM1-2-HR</td><td>Cooling degree days (4)</td></tr>
<tr><td>Extreme heat</td><td>Heatwave events (12)
Heatwave days (12)
Tropical nights</td></tr>
</table>

Wet and Dry	Mean precipitation	MRI-ESM2-0 UKESM1-0-LL	Precipitation intensity index
	Heavy precipitation and pluvial flood		(Very) Heavy precipitation days (2) (Very) Wet days (2)
	Aridity		Consecutive dry days
	Hydrological drought	Three global hydrological datasets (H.08, LPJmL, MATSIRO) each of which have been forced by the five ESM scenario datasets above.	Drought intensity (2) Seasonality (2)* Inter-annual variability (2)*

* These two indices are not necessarily related to hydrological drought, although this is the CID category into which they best fit given that they represent the seasonal and annual variability of water resources.

As described in (Werning et al., 2024b), the dataset was consistently calculated for 31-year global warming levels of 1.2 (current day) and 1.5-3.5 °C (at 0.5 °C intervals) above the pre-industrial control period , based on gridded maps at 0.5° spatial resolution. The indicators in the dataset by GWL represent the mean of the 31 annual values. Given the multi-model setup comprising ISIMIP3b scenarios (SSP126, SSP370 and SSP5858) (Frieler, 2024; O'Neill et al., 2016), the dataset is available as ensemble statistics for each GWL. Here, the multi-model median is primarily used, although the workflow can take ensemble members or ensemble percentiles (as explored in section 2.6, Figure 5 and SI 3.3). For each GWL, the CID indices are available as absolute values, percentage difference to the reference period (1974-2004), or as a comparable 0-6 impact score. The impact score extends previous approaches (Byers et al., 2018), but takes into account both the absolute value of the index and the relative change experienced (Werning et al., 2024b), currently showcased on the ENGAGE project Climate Solutions Explorer (www.climate-solutions-explorer.eu). The CID indices are also spatially aggregated to various regional units, including country, IPCC and R10 regions, and are available as table data. Population and land area exposure metrics above a threshold value for each CID index aggregated for the regional units are also available. In the case of population, which changes through time according to the SSP scenario, an additional dimension is required, in order to compare the population exposure in future years for different GWLs.

Table 2.Overview of the dimensions of climate impacts database (Werning et al., 2024a, 2024b) used to demonstrate the emulation.

	As tested	**Comments**
Input datasets	Climate impact driver indices & exposure metrics data by GWLs (Werning et al., 2024a)	Gridded and table data. - 0.5° spatial resolution, global coverage - Table data calculates exposure of land area or population by SSP, also through time and at GWLs, above impact thresholds, following approaches in (Byers et al., 2018; Werning et al., 2024b)

Global Warming Levels (GWLs)	1.2, 1.5, 2.0, 2.5, 3.0, 3.5 °C,	Degrees Celsius above the pre-industrial control period as defined by the ISIMIP3 protocol, calculated for 31-year time-slices. More granular GWLs as input data would further reduce uncertainties around non-linear responses between these levels, although is expected to be comparatively small compared to other uncertainties.
Ensemble statistics	Median, *p5*, *p95*	For each CID index and GWL, percentiles across the ensemble of models and scenarios are available (5, 25, 50, 75, 95).
Socioeconomic pathways	SSPs 1-5	Applicable when assessing regionally-aggregated metrics relating to population exposure
Population exposure	Gridded SSP population projections	Original gridded downscaled SSP population projections (Jones and O'Neill, 2016; KC and Lutz, 2017), re- scaled to the latest version (KC et al., 2024; Werning, 2024) are overlaid with the CID indices data (Werning et al., 2024b).
Exposure threshold	≥3	Pixels with a score ≥3 are considered exposed to moderate climate impacts as per this method (Werning et al., 2024b, 2024a).
Exposure aggregation spatial units	Countries IPCC climate zone regions R5, R6 or R10 regions	For 225 countries and states (Perrette, 2023) For 44 IPCC regions as used in AR6 (Iturbide et al., 2020) For 5, 6 or 10 common global regions, as used by the IAMC and IPCC (IPCC, 2022)
Spatial aggregation methods	Median, Mean Land-area weighted Population weighted	Median and mean take the value across the pixels, with no weighting. Land-area weighted mean considers the area per 0.5° pixel on a quadrilinear grid, which reduces pixel areas towards the poles. Static through time. Population weighted mean considers the changing spatial and temporal distribution of a population within an aggregation unit.

2.4 Multi-index lookup

Taking a GMT pathway through time, e.g. from 2020 to 2100, each temperature in the timeseries is mapped to the interpolated CID index and exposure metric database using multi-dimensional index look-up. This is primarily based on the CID index and GMT, and additionally year and SSP (or other dimensions) for cases when, for example, population exposure is assessed in the region-aggregated data (Figure 2). This produces two main output products (Figure 1, Figure S 4,) at 5-year or decadal timesteps, consistent with the GMT pathway of the IAM pathway. The first (Figure S 4, left) is gridded maps of the CID indices through time, provided in a spatially gridded netCDF format at 0.5° resolution, the resolution consistently used by ISIMIP. The second output product (Figure S 4, right) is data tables in the IAMC format, that aggregate impacts exposure metrics by spatial units through time, e.g., sum of population exposed to heatwave events for each country in the world. These tabular outputs of indicators can then be easily appended to the IAM output results or used as input data.

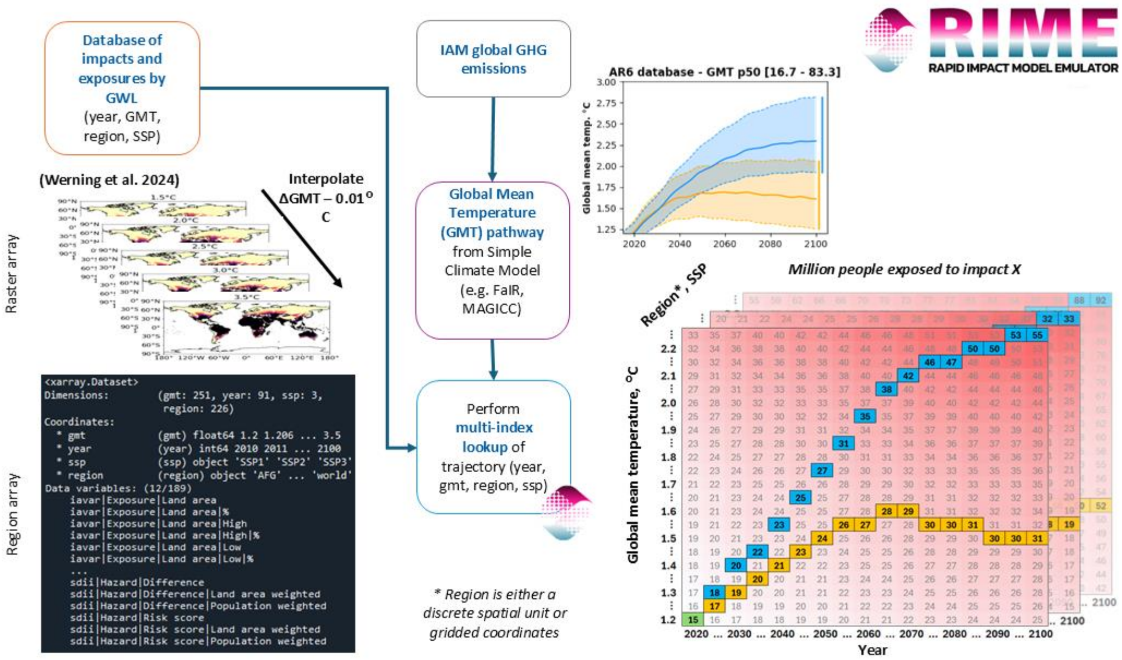

Figure 2. Schematic illustrating the data processing steps. The input datasets (either raster or region array) of CID indices and exposure metrics by Global Warming Level are linearly interpolated to a high resolution, and may include other dimensions, e.g., SSP, season, aggregation method. From this the Global Mean Temperature pathway of a global emissions scenario is used in a multi-index lookup to produce the CID index and exposure metrics values through time consistent with the GMT pathway of the scenario.

2.5 Implementation

The open-source software is implemented in Python (Rossum and Drake, 2010) and uses, amongst others, the python packages *pyam* (Huppmann et al., 2021) and *pandas* (The pandas development team, 2024) for table data, *xarray* (Hoyer and Hamman, 2017) for n-dimensional arrays including gridded climate data, and *dask* (Rocklin, 2015) for lazy and parallelized computation. Pyam is a package for analysis, manipulation and visualization of structured data, developed and used by the integrated assessment and energy systems modelling communities. Developed on top of pandas, pyam handles the input and output table-based datasets and ensures conformity and consistency with the IAMC data model. Xarray is used for handling n-dimensional arrays, primarily from the spatially gridded impacts data typically stored in netCDF format and is commonly used in climate research. The climate impacts input database, which could be 10s of GBs in size, also derives from tabular data but is stored as netCDF data and accessed using xarray and dask. Combined with dask, xarray handles the “lazy”, as needed reading and computation of such large datasets. Dask is also used explicitly in some of the core functions, to parallelize the processing of either multiple scenarios or indicators.

2.6 Characterization of uncertainty

The default mode of RIME takes a single GMT pathway as input, and provides a corresponding output based on the climate input database. Various use cases for exploring uncertainty are envisaged, however this depends on the input data available, not specifically the emulator (Table 3). In our default use case using the Werning et al. 2024a datasets, all cases in Table 3 are possible, although the default use case is to use the 50th percentile global mean temperature with multi-model ensemble medians across climate and impact models, with SSP2.

Table 3. Uncertainty categories and examples that can be considered in emulation. This possibility depends however on the input datasets available, not specifically this emulator.

Uncertainty Source	Examples	Description	Available in Werning et al. 2024a
Full range climate model sensitivity (exogenous)	Percentiles, e.g. p5, p17, p25, p33, p50, p67, p75, p83, p95	Full range climate uncertainty, such as from the CMIP6 range assessed by IPCC WGI and used in SCMs like FaIR and MAGICC, can be explored by using GMT pathways at different percentiles as input.	Not applicable
Climate model ensemble members	GFDL-ESM4, IPSL-CM6A-LR, MPI-ESM1-2-HR, ...	Ensemble member uncertainty through comparing results from individual model runs, for example the 5 ESMs used by ISIMIP, or different members from the same ESM.	Yes
Climate forcing scenario	SSP1-26, SSP3-70, SSP5-85	Forcing scenario uncertainty, whereby even for the same ESM and global warming level, different scenarios will have slightly different results.	Yes
Impact model	H.08, LPJmL, MATSIRO, CLM, CWatM, JULES, ORCHIDEE, …	Multiple impact models, e.g. hydrological or dynamic growth vegetation models, for a given climate will have differences, which is often larger than climate model and forcing uncertainties.	Yes
Socioeconomic scenario	SSP1, SSP2, SSP3,…	Different socioeconomic scenarios may be represented in an impact model, or in exposure and vulnerability calculations. Given its importance in climate impacts and risk assessment, within RIME this is an explicitly coded dimension similar to that of GMT.	Yes

Each CID index and its associated uncertainties will vary by region. Some indicators or regions exhibit a fairly monotonic response to increasing global mean temperature, while others show little or no clear trend. To help users identify where indicators can be meaningfully emulated across GWLs, the Pearson correlation coefficient can be calculated between index values, regions and GWLs (from 1.2 to 3.5 °C) using the multi-model ensemble median as well as the 5th and 95th percentiles (Table 4). Pearson's *r* provides a simple, unitless measure of the direction and consistency of the relationship, making it suitable for screening diverse indicators with varying units. While it does not quantify the rate of change, it efficiently highlights indicators and regions with robust and consistent trends, regardless of the magnitude of change, and can be applied to both gridded data and aggregated regions.

Table 4: Trend classification for the R10 regions and a selection of CID indices. A + indicates a statistically significant positive trend (Pearson coefficient >= 0.8, p value < 0.05), a – indicates a statistically significant negative trend (Pearson coefficient <= -0.8, p value < 0.05), a . denotes no significant trend. Trends are shown for the 5th percentile, median, and 95th percentile of the multi-model ensemble, in that order. For example, '+++' indicates a significant positive correlation across all three ensemble percentiles.

Indicator/ Region	Cooling degree days (24 °C)	Heatwave events (5 days, 99th perc.)	Heatwave days (5 days, 99th perc.)	Tropical nights	Consecutive dry days	Very heavy precipitation days	Very wet days	Precipitation intensity index	Drought intensity (discharge)
Latin America & Caribbean	+++	+++	+++	+++	+.+	...	+++	.+.	+++
South Asia	+++	+++	+++	+++	-..	..+	+++	..+	+.+
Sub-Saharan Africa	+++	+++	+++	+++	...	+.+	.++	+.+	++.
Centrally-planned Asia	+++	+++	+++	+++	---	+++	+++	+++	.++
Middle East	+++	+++	+++	+++	-..	.++	.++	-+.	++.
Eastern and Western Europe	+++	+++	+++	+++	+++	+..	++.	+++	+++
North America	+++	+++	+++	+++	---	+++	+++	+++	+.+
Other countries of Asia	+++	+..	+++	+++	...	+.+	+++	+++	+.-
Pacific OECD	+++	+++	+++	+++	...	+..	++.	..+	+++
Reforming Economies of Eastern Europe and the Former Soviet Union	+++	+++	+++	+++	---	++.	+++	+++	.+.

3 Illustrative results

To illustrate the potential of the emulator, results are presented using two previously unseen emissions scenarios from Working Group III of the IPCC 6th Assessment Report, identified as "Illustrative Pathways". The Moderate Action (ModAct) pathway assumes limited mitigation efforts, exceeding 1.95 °C and 2.69 °C global mean temperature with 50% likelihood in 2050 and 2100, respectively. This is comparable to the 2.7 °C expected under current policies and action by the November 2024 Climate Action Tracker. The Shifting Pathways (SP) scenario is an ambitious mitigation pathway that also assumes substantial progress on the Sustainable Development Goals, reaching 1.51 °C in 2050 and bringing temperatures back down to 1.17 °C by 2100.

Nine CID indices from the Werning et al. 2024b dataset are chosen for the purpose of projecting climate impacts from these pathways, shown in Figure 3 for 2050 in comparison to simulated 2020. Further figures for a wider set of CID indices are available in the Supporting Information (Figure S 1, Figure S 2, Figure S 3).

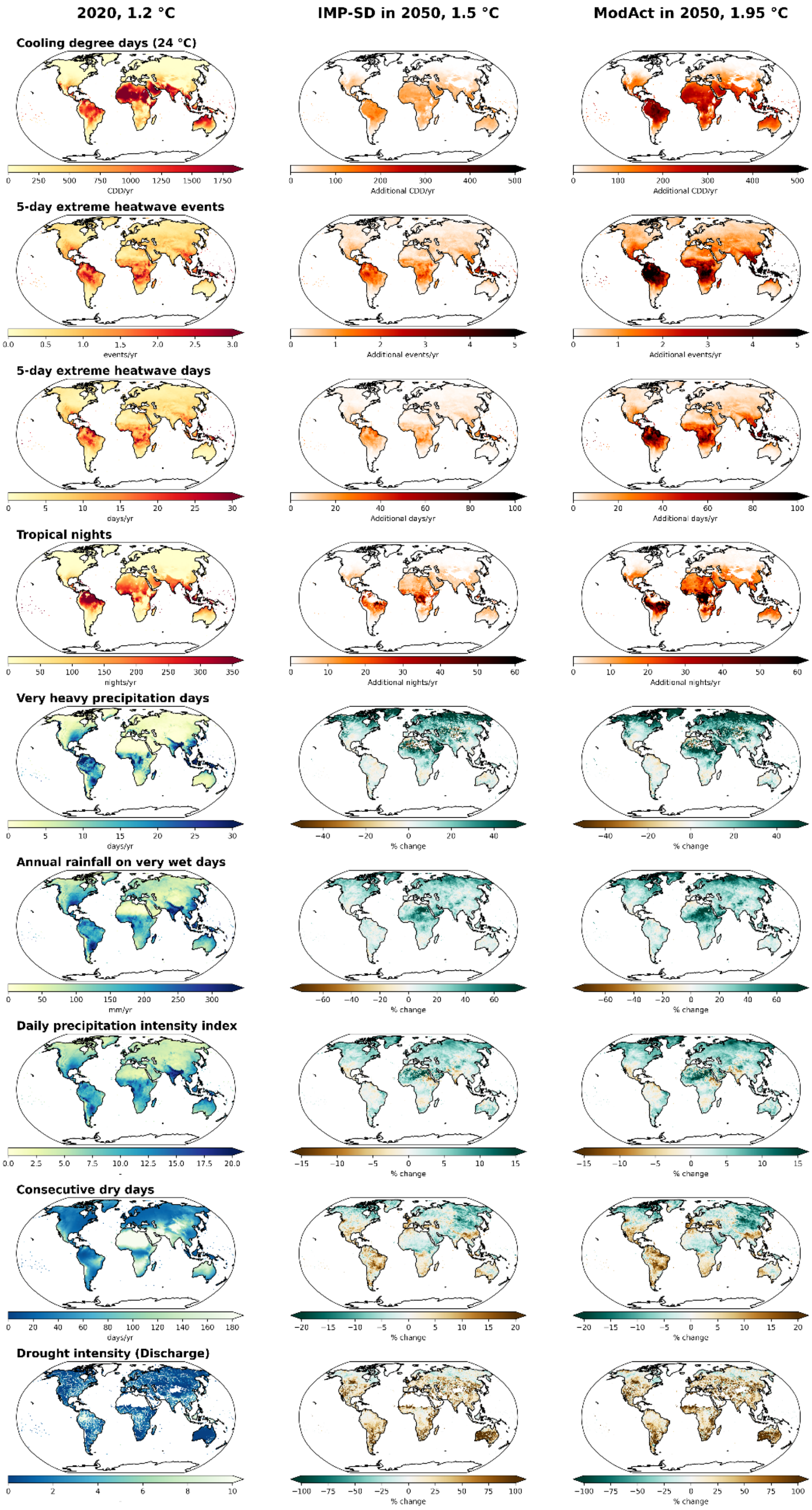

Figure 3. Emulated CID indices maps for 2020 (left column) and two (unseen) mitigation scenarios in 2050 for 9 indicators. In the centre and right columns for 2050, the Heat and Cold indices are shown as additional difference from

2020, whilst the Wet and Dry indices are shown as percentage change. Desert and ice sheet areas are masked out in white for drought intensity.

Similar results from the same dataset aggregated to regions can be used to explore, for example, population or land area weighted indices or exposure to these indices above thresholds (Werning et al., 2024b) (Figure 4). In such cases, the emulation is done directly on the tabular region array data, i.e. where exposure metrics per region has been aggregated a priori and form part of the input dataset. This could therefore be, for example, by country, climate zones, IPCC or IAM regions - any formulation, even if non-contiguous that can be defined according to the spatial grid.

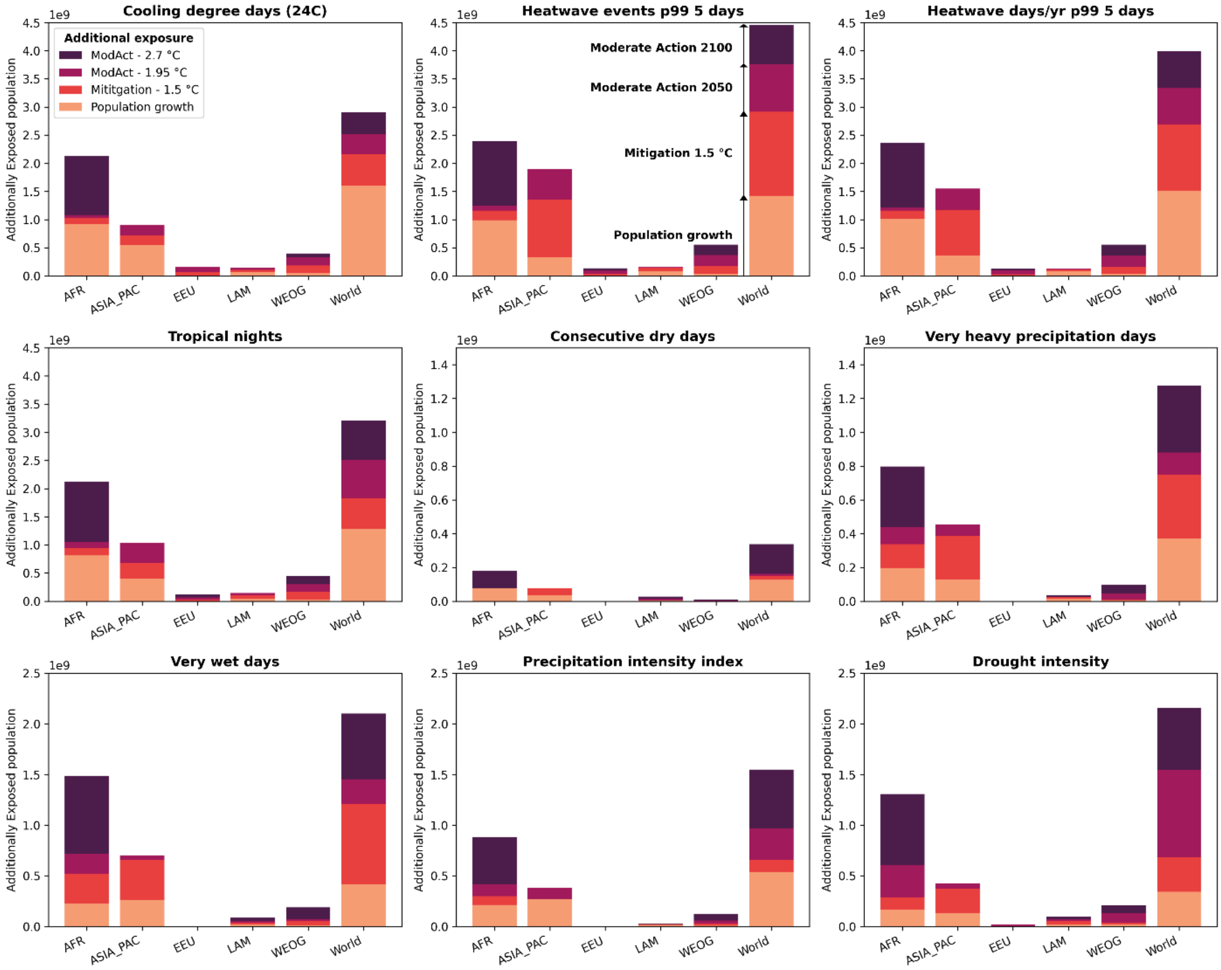

Figure 4. Regionally aggregated results for five UN and World regions showing the additional population exposure for nine CID index exposure metrics as driven by population growth (SSP2 in 2050) and climate change, compared to 2020 (1.2 °C). By 2050, population growth in currently exposed regions is substantial, with additional people exposed in the mitigation pathway at 1.5 °C. The Moderate Action pathway exacerbates this further, approximately doubling those exposed compared to mitigation at 1.5 °C in 2050. By 2100 at 2.7 °C the effects are even larger, despite the fact that by this point population in most regions is lower than in 2050. N.B. different y-axis limits.

The additionally exposed population is not only dependent on the different emission scenarios, but also varies with socioeconomic scenario and climate model sensitivity. Figure 5 shows a decomposition of these three different types of uncertainty for a selection of indicators, using the full range of SSP population projections and a selection of emissions scenarios and MAGICC percentiles. The chosen emissions scenarios include a range of climate outcomes and illustrative scenarios selected for the IPCC AR6 of WGIII to span a large range of climate outcomes up to 3.5 °C (Riahi et al., 2022). For the MAGICC percentiles, all percentiles available in the AR6 Scenarios Database are used (Byers et al., 2022) (Table S 5).

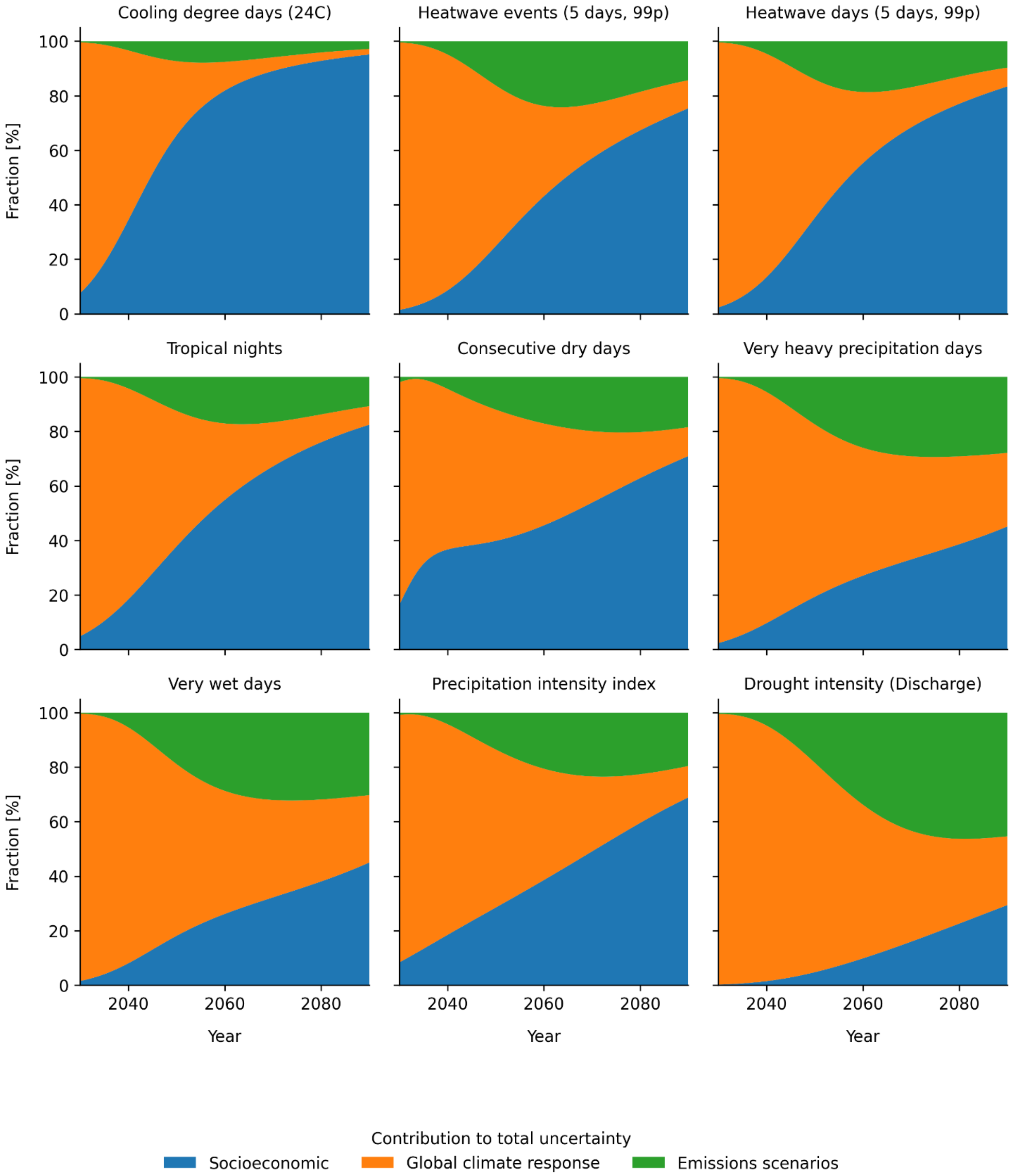

Figure 5: Relative contribution of different sources of uncertainty for the globally exposed population and a selection of CID indices.

The relative contribution of the three sources of uncertainty changes throughout the century. While the global climate model sensitivity expressed by the different MAGICC percentiles dominate at the beginning of the century for all indices, it rapidly declines after the middle of the century, especially for the Heat and Cold indices. The relative contribution of the socioeconomic scenarios to the total uncertainty, i.e. differences in population projections, shows the opposite trend and steadily increases throughout the century, also with a more rapid increase for the Heat and Cold indices, and becomes the dominant source of uncertainty by the end of the century. While the relative contribution of the emissions scenarios also increases in the first half of the century, it shows the smallest variation compared to the other two sources and starts to decrease again towards the end of the century. The contributions of the different sources of uncertainty also vary depending on the considered region. For the EU, for example, the uncertainty introduced by the different socioeconomic scenarios still increases with time, but for most indices stays below 5% (Figure S 6), given that population differences between the SSP scenarios is not large. Conversely for Sub-Saharan Africa, it is the dominant factor, contributing to more than 90% of the total uncertainty at the end of the century given the large differences in population development projections (Figure S 7). We acknowledge that RIME in its current form does not account for regional climate (impact) uncertainty (Pfleiderer et al., 2025), which is an important area for future development.

4 Discussion and roadmap for development

Based on the current features presented, here we outline some limitations and directions of future development. Broadly, this covers the topics of scenario ensemble assessment, representation of uncertainties and natural variability, overshoot scenarios, input dataset evaluation, and exploration of results.

Approaches to extend uncertainty assessment, across climatic, socioeconomic and scenario dimensions, are possible. Exposure and vulnerability scenarios, for example through combining gridded SSP-based data on population (as in (Werning et al., 2024b)) with data on income levels, can be used to assess socioeconomic drivers of climate risk. As shown in Figure 5, in terms of population exposure socioeconomic uncertainty late in the century is substantial particularly in developing regions. Another area, likely of interest to IPCC WGIII, will be assessing ranges of impacts across subsets of mitigation scenarios, to help answer questions like 'How does the range of climate impacts expected for "1.5 °C (>50%) with no or low overshoot" scenarios compare to a group of "likely below (>67%) 2 °C" scenarios '?

In discussing climate uncertainty, it is important to distinguish between (1) parametric uncertainty in the climate system (e.g., climate sensitivity, aerosol forcing), which can be explored through probabilistic GMT pathways from SCMs as was done with MAGICC percentiles, and (2) internal variability—natural, unforced fluctuations such as year-to-year ocean-atmosphere dynamics—which is not represented in RIME's current implementation.

RIME's inputs are based on 31-year multi-model ensemble means for each global warming level (GWL), consistent with standard time-slice methodology and pattern scaling assumptions. This averaging smooths out internal variability and produces a robust signal of the forced response. While technically possible to extract annual values or extremes from within a time slice, such approaches risk introducing artefacts, particularly when users misinterpret interannual fluctuations in global mean temperature as meaningful variation in climate impact indicators. To avoid this, RIME defaults to 5-year timesteps, in alignment with typical IAM scenario resolution.

Further development will combine climate forcing and model uncertainties in a fully probabilistic manner, advancing what has been presented here (Table 3, Table S 3, Table S 4) (Schwind, 2025). Exploring these uncertainties is already feasible through control of input datasets (section 2.6, Table 3) and comparing sources (Figure 5). While advanced emulators such as STITCHES or MESMER include internal variability through resampling or stochastic emulation, they rely on access to full ESM archives or bespoke calibration steps, differing from RIME's lightweight, time-slice based approach. Differentiating forcing scenario characteristics (e.g., aerosol levels) may also be important as pattern scaling behaviour has been shown to vary accordingly (Goodwin et al., 2020).

An important limitation arises when global mean temperature (GMT) stabilizes within the resolution of RIME's interpolation (default 0.05 °C). In such cases, RIME will return constant values for a given indicator, implicitly assuming a steady-state climate. While this behaviour aligns with the time-slice methodology used in the input data—where each GWL reflects average conditions over a 31-year window—it is a simplification. Furthermore, uncertainties about how climate impacts play out in temperature overshoot pathways means caution is required when assessing impacts post-peak warming (Schleussner et al., 2024). Due to potential hysteresis in climate and impact system responses (Kim et al., 2022), impacts during the post-peak phase may not mirror those at equivalent warming levels on the way up. Thus, RIME is set by default to exclude years where GMT falls more than 0.15 °C below the peak temperature. A more accurate overshoot treatment would separate pre- and post-peak temperature impacts databases. To do this requires however, more overshoot scenario runs from ESM and impacts models, importantly spanning a number of peak and decline temperature ranges, e.g. peaking at 1.5, 2, 2.5, and 3 °C. Thus, caution is needed with temperature overshoot scenarios or those with high aerosol emissions, where regionalised impacts pre- and post-peak are likely to be different (Schleussner et al., 2024; Schwaab et al., 2024; Shiogama et al., 2023).

The quality of data inputs is important, and users should be aware of impact model limitations. ISIMIP has potentially many impact models and indicators that could be emulated with RIME, and while comprehensive and harmonized, they have documented limitations. For example, some impact models underestimate the occurrence of large fires (Burton et al., 2024) or fail to adequately capture the impacts of extremes on crop yields and other variables (Schewe et al., 2019). The current implementation includes basic diagnostic tools for evaluation of input and output datasets. Determining how the input dataset responds to changes in global warming level at the gridpoint and regional level can be done using the functions demonstrated but could be further advanced, for example, through error metrics that decompose the internal variability (Tebaldi et al., 2020). Further checks on input temperature pathway data, for example checking for high levels of aerosol forcing which is a typical output of SCMs, could be used for screening for and indicating (low) confidence in regional results.

Lastly, although RIME was initially designed to complement IAM scenarios and facilitate integration between impacts and mitigation communities, such as between WGII-WGIII in the IPCC context, its design as a modular, open-source tool supports broader uses. A key focus going forward will be the development of more user-friendly results dashboards. The current interactive HTML dashboard displays zoomable maps for multiple scenarios or indicators. Future versions will include more selectable options, such as different timesteps, regional aggregations, distributions, and uncertainty ranges. National or regional dashboards could further broaden usability for diverse analytical and decision-making contexts. Further plans also aim to integrate this type of workflow into scenario post-processing routines, such that CID indices of emissions scenarios can be evaluated online on-the-fly, for example for online scenario databases like the Scenarios Compass Initiative (https://scenariocompass.org/). This broader applicability reflects our intention to support more inclusive, interdisciplinary engagement with climate impact information.

5 Conclusions

The initial setup of RIME provides climate impact drivers aligned with timeseries of global mean temperatures from IAM scenarios. Using established global warming level approaches, we demonstrate the rapid post-processing use case allowing ensembles of global temperature pathways, such as those from AR6 scenarios database (Byers et al., 2022) used by the IPCC, to be accompanied by a new suite of climate impacts and risk information. The approaches are computationally cheap and straightforward to apply, noting that they will not be suitable, in the current form, for certain use cases involving overshoot or impacts with a long memory such as sea-level rise or glacier loss.

Example results using a database of climate impacts driver indices are presented for two "Illustrative Pathways" from the IPCC AR6 WGIII report. They illustrate use of the RIME software package and estimation of climate impacts for unseen warming trajectories, at gridded and regionally aggregated resolutions. While climate uncertainties are the primary concern through mid-century, our results indicate that socio-economic factors such as population growth may become the dominant drivers of risk by the end of the century. Methods for representing and evaluating regional uncertainties were introduced and explored, with varied success depending on the CID index and region in question. Additional evaluation with more indices, in particular from impact models such as for hydrology and crops, will be the focus of further developments in the software.

The approach bridges a key gap between IPCC WGII and WGIII assessments, connecting the impacts and mitigation communities, respectively, and moves beyond the constraints of RCP pathways enabling a flexible and rapid impacts assessment. The approach is also well-suited for enabling the flexible representation of climate impacts in IAMs, either as pre-processing tool or as an endogenized module.

Code & data availability

The RIME package is available under an open-source GPL-3.0 license at https://github.com/iiasa/rime. A Zenodo repository of scripts and data for reproducing the analysis and figures in this manuscript is available at https://doi.org/10.5281/zenodo.15728371. The pre-processing steps requires the data used from (Werning et al., 2024a) available at https://doi.org/10.5281/zenodo.13753537 .

Acknowledgements

The authors thank the two reviewers for constructive and valuable recommendations. The authors acknowledge funding from the European Union under grant agreements 101081369 (SPARCCLE), 821371 (ENGAGE) for the initial work on the emulator and development of the datasets that underpin the analysis, and Climate Works Foundation project that funds the Network for Greening the Financial System Workstream on Scenario Design and Analysis. Additionally, the authors acknowledge the ISIMIP project (www.isimip.org) and model teams upon which the data is based.

References:

Allen, M.R., Frame, D.J., Huntingford, C., Jones, C.D., Lowe, J.A., Meinshausen, M., Meinshausen, N., 2009. Warming caused by cumulative carbon emissions towards the trillionth tonne. Nature 458, 1163–1166. https://doi.org/10.1038/nature08019

Beusch, L., Gudmundsson, L., Seneviratne, S.I., 2020. Emulating Earth system model temperatures with MESMER: from global mean temperature trajectories to grid-point-level realizations on land. Earth Syst. Dyn. 11, 139–159. https://doi.org/10.5194/esd-11-139-2020

Burton, C., Lampe, S., Kelley, D.I., Thiery, W., Hantson, S., Christidis, N., Gudmundsson, L., Forrest, M., Burke, E., Chang, J., Huang, H., Ito, A., Kou-Giesbrecht, S., Lasslop, G., Li, W., Nieradzik, L., Li, F., Chen, Y., Randerson, J., Reyer, C.P.O., Mengel, M., 2024. Global burned area increasingly explained by climate change. Nat. Clim. Change 14, 1186–1192. https://doi.org/10.1038/s41558-024-02140-w

Byers, E., Gidden, M., Leclere, D., Balkovic, J., Burek, P., Ebi, K., Greve, P., Grey, D., Havlik, P., Hillers, A., Johnson, N., Kahil, T., Krey, V., Langan, S., Nakicenovic, N., Novak, R., Obersteiner, M., Pachauri, S., Palazzo, A., Parkinson, S., Rao, N.D., Rogelj, J., Satoh, Y., Wada, Y., Willaarts, B., Riahi, K., Leclère, D., Balkovic, J., Burek, P., Ebi, K., Greve, P., Grey, D., Havlik, P., Hillers, A., Johnson, N., Kahil, T., Krey, V., Langan, S., Nakicenovic, N., Novak, R., Obersteiner, M., Pachauri, S., Palazzo, A., Parkinson, S., Rao, N.D., Rogelj, J., Satoh, Y., Wada, Y., Willaarts, B., Riahi, K., 2018. Global exposure and vulnerability to multi-sector development and climate change hotspots. Environ. Res. Lett. 13, 055012. https://doi.org/10.1088/1748-9326/aabf45

Byers, E., Krey, V., Kriegler, E., Riahi, K., Schaeffer, R., Kikstra, J., Lamboll, R., Nicholls, Z., Sandstad, M., Smith, C., van der Wijst, K., Lecocq, F., Portugal-Pereira, J., Saheb, Y., Stromann, A., Winkler, H., Auer, C., Brutschin, E., Lepault, C., Müller-Casseres, E., Gidden, M., Huppmann, D., Kolp, P., Marangoni, G., Werning, M., Calvin, K., Guivarch, C., Hasegawa, T., Peters, G., Steinberger, J., Tavoni, M., van Vuuren, D., Al -Khourdajie, A., Forster, P., Lewis, J., Meinshausen, M., Rogelj, J., Samset, B., Skeie, R., 2022. AR6 Scenarios Database. https://doi.org/10.5281/zenodo.7197970

Dorheim, K., Gering, S., Gieseke, R., Hartin, C., Pressburger, L., Shiklomanov, A.N., Smith, S.J., Tebaldi, C., Woodard, D.L., Bond-Lamberty, B., 2024. Hector V3.2.0: functionality and performance of a reduced-complexity climate model. Geosci. Model Dev. 17, 4855–4869. https://doi.org/10.5194/gmd-17-4855-2024

Eyring, V., Bony, S., Meehl, G.A., Senior, C.A., Stevens, B., Stouffer, R.J., Taylor, K.E., 2016. Overview of the Coupled Model Intercomparison Project Phase 6 (CMIP6) experimental design and organization. Geosci. Model Dev. 9, 1937–1958. https://doi.org/10.5194/gmd-9-1937-2016

Forster, P.M., Smith, C., Walsh, T., Lamb, W.F., Lamboll, R., Cassou, C., Hauser, M., Hausfather, Z., Lee, J.-Y., Palmer, M.D., von Schuckmann, K., Slangen, A.B.A., Szopa, S., Trewin, B., Yun, J., Gillett, N.P., Jenkins, S., Matthews, H.D., Raghavan, K., Ribes, A., Rogelj, J., Rosen, D., Zhang, X., Allen, M., Aleluia Reis, L., Andrew, R.M., Betts, R.A., Borger, A., Broersma, J.A., Burgess, S.N., Cheng, L., Friedlingstein, P., Domingues, C.M., Gambarini, M., Gasser, T., Gütschow, J., Ishii, M., Kadow, C., Kennedy, J., Killick, R.E., Krummel, P.B., Liné, A., Monselesan, D.P., Morice, C., Mühle, J., Naik, V., Peters, G.P., Pirani, A., Pongratz, J., Minx, J.C., Rigby, M., Rohde, R., Savita, A., Seneviratne, S.I., Thorne, P., Wells, C., Western, L.M., van der Werf, G.R., Wijffels, S.E., Masson-Delmotte, V., Zhai, P., 2025. Indicators of Global Climate Change 2024: annual update of key indicators of the state of the climate system and human influence. Earth Syst. Sci. Data 17, 2641–2680. https://doi.org/10.5194/essd-17-2641-2025

Frieler, K., 2024. Scenario Set-up and the new CMIP6-based climate-related forcings provided within the third round of the Inter-Sectoral Intercomparison Project (ISIMIP3b, group I and II). Geosci. Model Dev. submitted.

Frieler, K., Meinshausen, M., Mengel, M., Braun, N., Hare, W., 2012. A Scaling Approach to Probabilistic Assessment of Regional Climate Change. https://doi.org/10.1175/JCLI-D-11-00199.1

Gasser, T., Ciais, P., Boucher, O., Quilcaille, Y., Tortora, M., Bopp, L., Hauglustaine, D., 2017. The compact Earth system model OSCAR v2.2: description and first results. Geosci. Model Dev. 10, 271–319. https://doi.org/10.5194/gmd-10-271-2017

Goodwin, P., Leduc, M., Partanen, A.-I., Matthews, H.D., Rogers, A., 2020. A computationally efficient method for probabilistic local warming projections constrained by history matching and pattern scaling, demonstrated by WASP–LGRTC-1.0. Geosci. Model Dev. 13, 5389–5399. https://doi.org/10.5194/gmd-13-5389-2020

Hoegh-Guldberg, O., Jacob, D., Taylor, M., 2018. Impacts of 1.5°C of Global Warming on Natural and Human Systems, in: Special Report, Intergovernmental Panel on Climate Change. pp. 175–181.

Hoyer, S., Hamman, J., 2017. xarray: N-D labeled Arrays and Datasets in Python 5, 10. https://doi.org/10.5334/jors.148

Huppmann, D., Gidden, M.J., Nicholls, Z., Hörsch, J., Lamboll, R., Kishimoto, P.N., Burandt, T., Fricko, O., Byers, E., Kikstra, J., Brinkerink, M., Budzinski, M., Maczek, F., Zwickl-Bernhard, S., Welder, L., Álvarez Quispe, E.F., Smith, C.J., 2021. pyam: Analysis and visualisation of integrated assessment and macro-energy scenarios. Open Res. Eur. 1, 74. https://doi.org/10.12688/openreseurope.13633.1

Integrated Assessment Modelling Consortium [WWW Document], 2024. . IAMC. URL https://www.iamconsortium.org/ (accessed 2.25.24).

Inter-Sectoral Impact Model Intercomparison Project [WWW Document], 2024. . ISIMIP. URL https://www.isimip.org/ (accessed 2.25.24).

IPCC, 2023. Climate Change 2023: Synthesis Report. Contribution of Working Groups I, II and III to the Sixth Assessment Report of the Intergovernmental Panel on Climate Change. IPCC, Geneva, Switzerland.

IPCC, 2022. Annex II: Definitions, Units and Conventions, in: Al Khourdaje, A., van Dieman, R., Lamb, W.F., Pathak, M., Reisinger, A., de la Rue du Can, S., Skea, J., Slade, R., Some, S., Steg, L. (Eds.), Climate Change 2022: Mitigation of Climate Change. Contribution of Working Group III to the Sixth Assessment Report of the Intergovernmental Panel on Climate Change. Cambridge University Press, Cambridge, UK and New York, NY, USA, pp. 1821–1840. https://doi.org/10.1017/9781009157926.021

Iturbide, M., Gutiérrez, J.M., Alves, L.M., Bedia, J., Cerezo-Mota, R., Cimadevilla, E., Cofiño, A.S., Di Luca, A., Faria, S.H., Gorodetskaya, I.V., Hauser, M., Herrera, S., Hennessy, K., Hewitt, H.T., Jones, R.G., Krakovska, S., Manzanas, R., Martínez-Castro, D., Narisma, G.T., Nurhati, I.S., Pinto, I., Seneviratne, S.I., van den Hurk, B., Vera, C.S., 2020. An update of IPCC climate reference regions for subcontinental analysis of climate model data: definition and aggregated datasets. Earth Syst. Sci. Data 12, 2959–2970. https://doi.org/10.5194/essd-12-2959-2020

James, R., Washington, R., Schleussner, C.-F., Rogelj, J., Conway, D., 2017. Characterizing half-a-degree difference: a review of methods for identifying regional climate responses to global warming targets. Wiley Interdiscip. Rev. Clim. Change 8, e457-n/a. https://doi.org/10.1002/wcc.457

Jones, B., O’Neill, B.C., 2016. Spatially explicit global population scenarios consistent with the Shared Socioeconomic Pathways. Environ. Res. Lett. 11, 84003. https://doi.org/10.1088/1748-9326/11/8/084003

KC, S., Lutz, W., 2017. The human core of the shared socioeconomic pathways: Population scenarios by age, sex and level of education for all countries to 2100. Glob. Environ. Change 42, 181–192. https://doi.org/10.1016/j.gloenvcha.2014.06.004

KC, S., Moradhvaj, Potancokova, M., Adhikari, S., Yildiz, D., Mamolo, M., Sobotka, T., Zeman, K., Abel, G., Lutz, W., Goujon, A., 2024. Wittgenstein Center (WIC) Population and Human Capital Projections - 2023. https://doi.org/10.5281/zenodo.10618931

Kikstra, J.S., Nicholls, Z.R.J., Smith, C.J., Lewis, J., Lamboll, R.D., Byers, E., Sandstad, M., Meinshausen, M., Gidden, M.J., Rogelj, J., Kriegler, E., Peters, G.P., Fuglestvedt, J.S., Skeie, R.B., Samset, B.H., Wienpahl, L., van Vuuren, D.P., van der Wijst, K.-I., Al Khourdajie, A., Forster, P.M., Reisinger, A., Schaeffer, R., Riahi, K., 2022. The IPCC Sixth Assessment Report WGIII climate assessment of mitigation pathways: from emissions to global temperatures. Geosci. Model Dev. 15, 9075–9109. https://doi.org/10.5194/gmd-15-9075-2022

Kim, S.-K., Shin, J., An, S.-I., Kim, H.-J., Im, N., Xie, S.-P., Kug, J.-S., Yeh, S.-W., 2022. Widespread irreversible changes in surface temperature and precipitation in response to CO2 forcing. Nat. Clim. Change 12, 834–840. https://doi.org/10.1038/s41558-022-01452-z

Kitsios, V., O’Kane, T.J., Newth, D., 2023. A machine learning approach to rapidly project climate responses under a multitude of net-zero emission pathways. Commun. Earth Environ. 4, 1–15. https://doi.org/10.1038/s43247-023-01011-0

Lange, S., 2019. Trend-preserving bias adjustment and statistical downscaling with ISIMIP3BASD (v1.0). Geosci. Model Dev. 12, 3055–3070. https://doi.org/10.5194/gmd-12-3055-2019

Lange, S., Volkholz, J., Geiger, T., Zhao, F., Vega, I., Veldkamp, T., Reyer, C.P.O., Warszawski, L., Huber, V., Jägermeyr, J., Schewe, J., Bresch, D.N., Büchner, M., Chang, J., Ciais, P., Dury, M., Emanuel, K., Folberth, C., Gerten, D., Gosling, S.N., Grillakis, M., Hanasaki, N., Henrot, A.-J., Hickler, T., Honda, Y., Ito, A., Khabarov, N., Koutroulis, A., Liu, W., Müller, C., Nishina, K., Ostberg, S., Müller Schmied, H., Seneviratne, S.I., Stacke, T., Steinkamp, J., Thiery, W., Wada, Y., Willner, S., Yang, H., Yoshikawa, M., Yue, C., Frieler, K., 2020. Projecting Exposure to Extreme Climate Impact Events Across Six Event Categories and Three Spatial Scales. Earths Future 8, e2020EF001616. https://doi.org/10.1029/2020EF001616

Lehner, F., Deser, C., 2023. Origin, importance, and predictive limits of internal climate variability. Environ. Res. Clim. 2, 023001. https://doi.org/10.1088/2752-5295/accf30

Masson-Delmotte, V., Zhai, P., Pirani, A., Connors, S.L., Péan, C., Berger, S., Caud, N., Chen, Y., Goldfarb, L., Gomis, M.I., others, 2021. Summary for policymakers, in: Climate Change 2021: The Physical Science Basis. Contribution of Working Group I to the Sixth Assessment Report of the Intergovernmental Panel on Climate Change. Cambridge University Press.

Meinshausen, M., Raper, S.C.B., Wigley, T.M.L., 2011. Emulating coupled atmosphere-ocean and carbon cycle models with a simpler model, MAGICC6 – Part 1: Model description and calibration. Atmospheric Chem. Phys. 11, 1417–1456. https://doi.org/10.5194/acp-11-1417-2011

Myhre, G., Kramer, R.J., Smith, C.J., Hodnebrog, Ø., Forster, P., Soden, B.J., Samset, B.H., Stjern, C.W., Andrews, T., Boucher, O., Faluvegi, G., Fläschner, D., Kasoar, M., Kirkevåg, A., Lamarque, J.-F., Olivié, D., Richardson, T., Shindell, D., Stier, P., Takemura, T., Voulgarakis, A., Watson-Parris, D., 2018.

Quantifying the Importance of Rapid Adjustments for Global Precipitation Changes. Geophys. Res. Lett. 45, 11,399-11,405. https://doi.org/10.1029/2018GL079474

Nath, S., Carreau, J., Kornhuber, K., Pfleiderer, P., Schleussner, C.-F., Naveau, P., 2024. MERCURY: A fast and versatile multi-resolution based global emulator of compound climate hazards. https://doi.org/10.48550/arXiv.2501.04018

Nath, S., Lejeune, Q., Beusch, L., Seneviratne, S.I., Schleussner, C.-F., 2022. MESMER-M: an Earth system model emulator for spatially resolved monthly temperature. Earth Syst. Dyn. 13, 851–877. https://doi.org/10.5194/esd-13-851-2022

Nicholls, Z.R.J., Meinshausen, M., Lewis, J., Gieseke, R., Dommenget, D., Dorheim, K., Fan, C.-S., Fuglestvedt, J.S., Gasser, T., Golüke, U., Goodwin, P., Hartin, C., Hope, A.P., Kriegler, E., Leach, N.J., Marchegiani, D., McBride, L.A., Quilcaille, Y., Rogelj, J., Salawitch, R.J., Samset, B.H., Sandstad, M., Shiklomanov, A.N., Skeie, R.B., Smith, C.J., Smith, S., Tanaka, K., Tsutsui, J., Xie, Z., 2020. Reduced Complexity Model Intercomparison Project Phase 1: introduction and evaluation of global-mean temperature response. Geosci. Model Dev. 13, 5175–5190. https://doi.org/10.5194/gmd-13-5175-2020

O'Neill, B.C., Tebaldi, C., van Vuuren, D.P., Eyring, V., Friedlingstein, P., Hurtt, G., Knutti, R., Kriegler, E., Lamarque, J.-F., Lowe, J., Meehl, G.A., Moss, R., Riahi, K., Sanderson, B.M., 2016. The Scenario Model Intercomparison Project (ScenarioMIP) for CMIP6. Geosci. Model Dev. 9, 3461–3482. https://doi.org/10.5194/gmd-9-3461-2016

Perrette, M., 2023. ISI-MIP/isipedia-countries (v2.6).

Pfleiderer, P., Frölicher, T.L., Kropf, C.M., Lamboll, R.D., Lejeune, Q., Capela Lourenço, T., Maussion, F., McCaughey, J.W., Quilcaille, Y., Rogelj, J., Sanderson, B., Schuster, L., Sillmann, J., Smith, C., Theokritoff, E., Schleussner, C.-F., 2025. Reversal of the impact chain for actionable climate information. Nat. Geosci. 18, 10–19. https://doi.org/10.1038/s41561-024-01597-w

Piontek, F., Müller, C., Pugh, T.A.M., Clark, D.B., Deryng, D., Elliott, J., De Jesus Colón González, F., Flörke, M., Folberth, C., Franssen, W., Frieler, K., Friend, A.D., Gosling, S.N., Hemming, D., Khabarov, N., Kim, H., Lomas, M.R., Masaki, Y., Mengel, M., Morse, A., Neumann, K., Nishina, K., Ostberg, S., Pavlick, R., Ruane, A.C., Schewe, J., Schmid, E., Stacke, T., Tang, Q., Tessler, Z.D., Tompkins, A.M., Warszawski, L., Wisser, D., Schellnhuber, H.J., 2014. Multisectoral climate impact hotspots in a warming world. Proc. Natl. Acad. Sci. U. S. A. 111, 3233–3238. https://doi.org/10.1073/pnas.1222471110

Quilcaille, Y., Gasser, T., Ciais, P., Boucher, O., 2023a. CMIP6 simulations with the compact Earth system model OSCAR v3.1. Geosci. Model Dev. 16, 1129–1161. https://doi.org/10.5194/gmd-16-1129-2023

Quilcaille, Y., Gudmundsson, L., Beusch, L., Hauser, M., Seneviratne, S.I., 2022. Showcasing MESMER-X: Spatially Resolved Emulation of Annual Maximum Temperatures of Earth System Models. Geophys. Res. Lett. 49, e2022GL099012. https://doi.org/10.1029/2022GL099012

Quilcaille, Y., Gudmundsson, L., Seneviratne, S.I., 2023b. Extending MESMER-X: a spatially resolved Earth system model emulator for fire weather and soil moisture. Earth Syst. Dyn. 14, 1333–1362. https://doi.org/10.5194/esd-14-1333-2023

Riahi, K., Schaeffer, R., Arango, J., Calvin, K., Guivarch, C., Hasegawa, T., Jiang, K., Kriegler, E., Matthews, R., Peters, G.P., Rao, A., Robertson, S., Sebbit, A.M., Steinberger, J., Tavoni, M., Van Vuuren, D.P., 2022. Mitigation pathways compatible with long-term goals. Clim. Change 2022 Mitig. Clim. Change Contrib.

Work. Group III Sixth Assess. Rep. Intergov. Panel Clim. Change. https://doi.org/10.1017/9781009157926.005

Rocklin, M., 2015. Dask: Parallel Computation with Blocked algorithms and Task Scheduling. Presented at the Python in Science Conference, Austin, Texas, pp. 126–132. https://doi.org/10.25080/Majora-7b98e3ed-013

Rossum, G. van, Drake, F.L., 2010. The Python language reference, Release 3.0.1 [Repr.]. ed, Python documentation manual / Guido van Rossum; Fred L. Drake [ed.]. Python Software Foundation, Hampton, NH.

Ruane, A.C., Vautard, R., Ranasinghe, R., Sillmann, J., Coppola, E., Arnell, N., Cruz, F.A., Dessai, S., Iles, C.E., Islam, A.K.M.S., Jones, R.G., Rahimi, M., Carrascal, D.R., Seneviratne, S.I., Servonnat, J., Sörensson, A.A., Sylla, M.B., Tebaldi, C., Wang, W., Zaaboul, R., 2022. The Climatic Impact-Driver Framework for Assessment of Risk-Relevant Climate Information. Earths Future 10, e2022EF002803. https://doi.org/10.1029/2022EF002803

Sandstad, M., Aamaas, B., Johansen, A.N., Lund, M.T., Peters, G.P., Samset, B.H., Sanderson, B.M., Skeie, R.B., 2024. CICERO Simple Climate Model (CICERO-SCM v1.1.1) – an improved simple climate model with a parameter calibration tool. Geosci. Model Dev. 17, 6589–6625. https://doi.org/10.5194/gmd-17-6589-2024

Schewe, J., Gosling, S.N., Reyer, C., Zhao, F., Ciais, P., Elliott, J., Francois, L., Huber, V., Lotze, H.K., Seneviratne, S.I., van Vliet, M.T.H., Vautard, R., Wada, Y., Breuer, L., Büchner, M., Carozza, D.A., Chang, J., Coll, M., Deryng, D., de Wit, A., Eddy, T.D., Folberth, C., Frieler, K., Friend, A.D., Gerten, D., Gudmundsson, L., Hanasaki, N., Ito, A., Khabarov, N., Kim, H., Lawrence, P., Morfopoulos, C., Müller, C., Müller Schmied, H., Orth, R., Ostberg, S., Pokhrel, Y., Pugh, T.A.M., Sakurai, G., Satoh, Y., Schmid, E., Stacke, T., Steenbeek, J., Steinkamp, J., Tang, Q., Tian, H., Tittensor, D.P., Volkholz, J., Wang, X., Warszawski, L., 2019. State-of-the-art global models underestimate impacts from climate extremes. Nat. Commun. 10, 1005. https://doi.org/10.1038/s41467-019-08745-6

Schleussner, C.-F., Ganti, G., Lejeune, Q., Zhu, B., Pfleiderer, P., Prütz, R., Ciais, P., Frölicher, T.L., Fuss, S., Gasser, T., Gidden, M.J., Kropf, C.M., Lacroix, F., Lamboll, R., Martyr, R., Maussion, F., McCaughey, J.W., Meinshausen, M., Mengel, M., Nicholls, Z., Quilcaille, Y., Sanderson, B., Seneviratne, S.I., Sillmann, J., Smith, C.J., Steinert, N.J., Theokritoff, E., Warren, R., Price, J., Rogelj, J., 2024. Overconfidence in climate overshoot. Nature 634, 366–373. https://doi.org/10.1038/s41586-024-08020-9

Schleussner, C.F., Lissner, T.K., Fischer, E.M., Wohland, J., Perrette, M., Golly, A., Rogelj, J., Childers, K., Schewe, J., Frieler, K., Mengel, M., Hare, W., Schaeffer, M., 2016. Differential climate impacts for policy-relevant limits to global warming: The case of 1.5 °c and 2 °c. Earth Syst. Dyn. 7, 327–351. https://doi.org/10.5194/esd-7-327-2016

Schöngart, S., Gudmundsson, L., Hauser, M., Pfleiderer, P., Lejeune, Q., Nath, S., Seneviratne, S.I., Schleußner, C.-F., 2024. Introducing the MESMER-M-TPv0.1.0 module: Spatially Explicit Earth System Model Emulation for Monthly Precipitation and Temperature. EGUsphere 1–51. https://doi.org/10.5194/egusphere-2024-278

Schwaab, J., Hauser, M., Lamboll, R.D., Beusch, L., Gudmundsson, L., Quilcaille, Y., Lejeune, Q., Schöngart, S., Schleussner, C.-F., Nath, S., Rogelj, J., Nicholls, Z., Seneviratne, S.I., 2024. Spatially resolved emulated annual temperature projections for overshoot pathways. Sci. Data 11, 1262. https://doi.org/10.1038/s41597-024-04122-1

Schwind, N., 2025. RIME-X: Emulating regional climate impact distributions using simple climate models and impact models, in: CL3.2.3 – Statistical and Physical Emulators for Climate Impacts. Presented at the EGU General Assembly 2025.

Shiogama, H., Fujimori, S., Hasegawa, T., Hayashi, M., Hirabayashi, Y., Ogura, T., Iizumi, T., Takahashi, K., Takemura, T., 2023. Important distinctiveness of SSP3–7.0 for use in impact assessments. Nat. Clim. Change 13, 1276–1278. https://doi.org/10.1038/s41558-023-01883-2

Smith, C.J., Forster, P.M., Allen, M., Leach, N., Millar, R.J., Passerello, G.A., Regayre, L.A., 2018. FAIR v1.3: a simple emissions-based impulse response and carbon cycle model. Geosci. Model Dev. 11, 2273–2297. https://doi.org/10.5194/gmd-11-2273-2018

Tebaldi, C., Armbruster, A., Engler, H.P., Link, R., 2020. Emulating climate extreme indices. Environ. Res. Lett. 15, 074006. https://doi.org/10.1088/1748-9326/ab8332

Tebaldi, C., Knutti, R., 2018. Evaluating the accuracy of climate change pattern emulation for low warming targets. Environ. Res. Lett. 13, 055006. https://doi.org/10.1088/1748-9326/aabef2

Tebaldi, C., Selin, N.E., Ferrari, R., Flierl, G., 2025. Emulators of Climate Model Output. Annu. Rev. Environ. Resour. 50. https://doi.org/10.1146/annurev-environ-012125-085838

Tebaldi, C., Snyder, A., Dorheim, K., 2022. STITCHES: creating new scenarios of climate model output by stitching together pieces of existing simulations. Earth Syst. Dyn. 13, 1557–1609. https://doi.org/10.5194/esd-13-1557-2022

The pandas development team, 2024. pandas-dev/pandas: Pandas. https://doi.org/10.5281/zenodo.10697587

van Vuuren, D., O’Neill, B., Tebaldi, C., Chini, L., Friedlingstein, P., Hasegawa, T., Riahi, K., Sanderson, B., Govindasamy, B., Bauer, N., Eyring, V., Fall, C., Frieler, K., Gidden, M., Gohar, L., Jones, A., King, A., Knutti, R., Kriegler, E., Lawrence, P., Lennard, C., Lowe, J., Mathison, C., Mehmood, S., Prado, L., Zhang, Q., Rose, S., Ruane, A., Schleussner, C.-F., Seferian, R., Sillmann, J., Smith, C., Sörensson, A., Panickal, S., Tachiiri, K., Vaughan, N., Vishwanathan, S., Yokohata, T., Ziehn, T., 2025. The Scenario Model Intercomparison Project for CMIP7 (ScenarioMIP-CMIP7)   EGUsphere 1–38. https://doi.org/10.5194/egusphere-2024-3765

Wells, C.D., Jackson, L.S., Maycock, A.C., Forster, P.M., 2023. Understanding pattern scaling errors across a range of emissions pathways. Earth Syst. Dyn. 14, 817–834. https://doi.org/10.5194/esd-14-817-2023

Werning, M., 2024. Gridded maps of global population scaled to match the 2023 Wittgenstein Center (WIC) Population projections. https://doi.org/10.5281/zenodo.13745063

Werning, M., Frank, S., Hooke, D., Nguyen, B., Rafaj, P., Satoh, Y., Wögerer, M., Krey, V., Riahi, K., van Ruivjen, B., Byers, E., 2024a. Climate Solutions Explorer - hazard, impacts and exposure data, v1.0. https://doi.org/10.5281/zenodo.13753537

Werning, M., Hooke, D., Krey, V., Riahi, K., Ruijven, B. van, Byers, E.A., 2024b. Global warming level indicators of climate change and hotspots of exposure. Environ. Res. Clim. 3, 045015. https://doi.org/10.1088/2752-5295/ad8300